Acta Scientific Microbiology (ISSN: 2581-3226)

Volume 7 Issue 2 February 2024

Research Article

Mid-infrared - A Laser Potentiator to Enhance the Potency of Antibiotics *In Vitro*

Umakanthan[1]*, Madhu Mathi[2], Umadevi[3] and Sivaramakrishnan[4]

[1]*Veterinary Hospital, Gokulam Annadhanam Temple Complex, Tamil Nadu, India*

[2]*Veterinary Hospital, Vadakupudhu Palayam Post, Tamil Nadu, India*

[3]*Assistant Professor, Department of Botany, The Standard Fireworks Rajaratnam College for Women, Sivakasi, Virudhunagar (Dt), Tamil Nadu, India*

[4]*Veterinary Assistant Surgeon, Veterinary Dispensary, Tamil Nadu, India*

***Corresponding Author:** Umakanthan, Veterinary Hospital, Gokulam Annadhanam Temple Complex, Tamil Nadu, India.

DOI: 10.31080/ASMI.2024.07.1349

Received: November 27, 2023

Published: January 25, 2024

Abstract

Antimicrobial potentiation can reduce dosage and cost while also reducing host stress. In general, potentiation is achieved to some extent through the combination of antimicrobials, but it is not always beneficial, particularly due to concerns about multi-drug resistance and economic issues. To favorably overcome these issues, we developed an approach in which irradiation with non-ionizing 2-6 µm mid-infrared (mid-IR) light increased the potency of antibiotics by severalfold. Different groups of antibiotics were treated with 2-6 µm mid-IR and challenged with different pathogens. We observed that antibiotic potency was enhanced by 5-173%. We developed a mid-infrared-generating atomizer (MIRGA). Through the agar well-diffusion method, a sensory expert panel test, and a variety of instrumentations, we deciphered that the mid-IR's effect on the irradiated antibiotics included changes in chemical bonding, configuration, atomic arrangement, and chemical compounds that are responsible for the enhanced potentiation. This technique is found to be safe, easily applicable, and economical, with a vast scope for the future potentiation of other pharmacological compounds as well.

Keywords: Antibiotics; 2-6 µm Mid-Infrared; Antibiotics Potentiation; Enhancement; Economy; Safe

Abbreviations

MIRGA: Mid-Infrared-Generating Atomizer; ZOI: Zone of Inhibition; MDR: Multi Drug Resistance; GC-MS: Gas Chromatography-Mass Spectrometry; PXRD: Powder X-ray Diffraction; FTIR: Fourier-Transform Infrared Spectroscopy; TEM: Transmission Electron Microscopy; 1H-NMR: Proton Nuclear Magnetic Resonance

Introduction

The development of bacterial resistance and the discovery of new drugs are always dynamic. Pair/triple combination of antibacterial therapy is in common now, but body physiology less compensates for their action [1-4]**.** The effects of a combination of antimicrobial compounds can be broadly classified as additive (the sum of the effect is equal to the addition of two or more individual compounds; i.e., 1+1 = 2), antagonistic (the sum of the effect is less than the addition of the individual compounds; 1 + 1 = <2), or synergistic (the sum of the effect is more than the addition of the individual compounds; 1 + 1 = >2). For each of the above effects, various researchers use different terminologies [5].

Several antibacterial combinations have been evaluated and are used for treating both human and animal diseases. However, reports indicate that combination therapy is favorable only for certain groups of patients and may lead to multidrug resistance (MDR) [6,7], in addition to being uneconomical. Therefore, increasing the potency of any particular antibiotic without changing the dose would be beneficial in reducing toxicity and MDR-related problems.

Being widely found in various medical applications, electromagnetic radiation, especially ultraviolet light, is an important avenue. Light-assisted antibiotics [8,9], although not fully studied, have been initiated to overcome the issue of bacterial resistance. Nearer to the UV lies the mid-infrared (mid-IR), which is the fingerprint region commonly used in biological applications [10]. To study mid-

IR as a potential laser adjuvant, we designed a mid-IR-generating atomizer, abbreviated as MIRGA, and applied this to potentiate the antibiotics that are commonly used against several virulent common bacterial pathogens. This paper discusses the positive outcomes of antibiotic potentiation with mid-IR and its mechanism in detail.

Materials and Methods

Mid-IR generating atomizer (MIRGA)

A 20 ml capacity polypropylene plastic atomizer of dimension 86 x 55 x 11 mm, orifice diameter 0.375 mm, ejection volume 0.062 ± 0.005 ml, ejection time 0.2 sec and average pressure 3900 pascal and cone liquid back pressure 2000 N/m^2 was designed and named MIRGA (patent no.:401387). It contained an inorganic water-based solution of molar mass 118.44 gm/mole. The chemical formulation of the solution is Sodium carbonate monohydrate, Sodium carbonate anhydrous, Potassium nitrate, Sodium chloride, and water. During spraying, approximately 1 µg weight of water as the mist is lost and the non-volatile material in the sprayed liquid is 153 mg/ml [11-13].

The solution contains an imbalanced ratio of the ions suspended in water in their fundamental state and can move as free particles (20ml contains approximately two sextillion cations and three sextillion anions). It has a very little background frequency of detectable disintegration which is less than that of cosmic events whereas even humans have more radioactivity (around 10 microns) [14,15]. Every time spraying emits 0.06ml which contains approximately seven quintillion cations and eleven quintillion anions. While spraying the MIRGA, the water-based ionic solution gets excited/ charged, which in turn leads to oscillation among the imbalanced ions [16], resulting in the emission of mid-IR light [17,18]. Though a low electromagnetic field exists between charged particles of the MIRGA's ionic solution, during spraying the induced oscillation between these charged particles produces mid-IR light [19-22].

From repeated trial and error experiments, we calibrated the design and average ejection pressure of the atomizer to 3900 pascals to obtain the desired fine mist, and minimize the evaporation rate by altering the pH and density of the solution. Following these fabrications, MIRGA is assembled to emit energy in the 2-6 µm mid-IR range upon spraying the presser given by the user. This was estimated using an FTIR (retro-reflector) interferometer instrument (Detector type D* [cm HZ1/2 - 1] MCT [2-TE cooled]) at Lightwind, Petaluma, California.

MIRGA spraying was externally done from a distance of 0.25 to 0.50 meters over the packaged antibiotic discs. This distance allowed the MIRGA solution to form ion clouds, which oscillated and generated 2-6µm mid-IR; closer spraying did not generate the mid-IR. The 2-6µm mid-IR penetrated the intervening packaging material and acted on the inside antibiotic discs [23]. A similar study using 'Universal Potentiator' has served as a primeval for the design of MIRGA.

Method I - Agar well diffusion

Some commonly used antibiotics (discs) and commonly encountered virulent bacteria (hospital isolated) were tested in this study. Nutrient agar/ Mueller-Hinton agar medium was used in the conducted agar well diffusion method (a modified method of [24] as below).

In a Petri dish with agar medium, we made 5 wells to accommodate antibiotic discs and marked the wells as C (control), 1, 2, 3, and 4. In the C well, an antibiotic-impregnated disc (e.g.,30 µg oxytetracycline) was placed. To study potentiation, four packets (1, 2, 3, and 4) of 30 µg oxytetracycline impregnated discs (each packet consisting of 50 discs) were sprayed with MIRGA at a distance of 0.25 - 0.50 meter towards the packets numbered 1, 2, 3 and 4 at a rate of 1, 2, 3 and 4 sprayings respectively. After spraying, one disc from each packet (1-4) was placed into the corresponding well (1-4). All the Petri dishes were inoculated with the same bacteria and incubated at 37° C for 12 hours. The zone of inhibition (ZOI) within each well was measured and compared between wells C, 1, 2, 3, and 4.

Each trial was repeated eight times with control. Many other such trials including control using different antibiotics against different bacterial isolates were done.

Method II - Sensory tests

Since some antibiotics are common and orally consumable, especially in veterinary therapy we as an initiative decided to subject them to sensory tests. The sensory evaluation of the 15 oxytetracycline samples based on the 9-point hedonic scale [25,26]: 1 - Dislike extremely, 2 - Dislike very much, 3 - Dislike moderately, 4 - Dislike slightly, 5 - Neither like nor dislike, 6 - Like slightly, 7 - Like moderately, 8 - Like very much, 9 - Like.

Fifteen packets of commercially available oxytetracycline powder were purchased, with each packet containing 100 gms. They were marked as C (control) and 1-14 numbers (trials). Packet C re-

ceived no spraying, whereas packets numbered 1-14 received 1-14 sprayings respectively, as in method I (from a distance of 0.25-0.50 meters). After spraying, each packet was subjected to a sensory expert panel test (n = 6).

Fourteen sprayings were given to oxytetracycline to determine the effect of an excessive number of MIRGA sprayings on antibiotics, as, in nature, the input of an excessive dose of electromagnetic waves should denature the receptors.

To assess the molecular level changes caused by mid-IR by which the potency of antibiotics was expected to be enhanced, the sprayed and non-sprayed samples e.g., oxytetracycline were trialed and subjected to some instrumentation tests.

Method III - Instrumental analysis

Based on the sensory scores, the control sample, 2 sprayed (sweetness enhanced), 6 sprayed (bitterness increased), and 12 sprayed (extremely increased bitterness and sweetness) samples were subjected to the below instruments to demonstrate,

- Chemical compound transformation: GC-MS: Agilent Technologies, 7820 GC system, 5977E MSD, Colomn DB-5, Over temp 100-270^{0}C, Detector MS, Flow rate 1.2, Carrier gas Helium
- Structural changes: PXRD: Rigaku RINT 2500 X-ray diffractometer (CuKα anode; λ = 1.541Å). Samples scanned at 40kV and 30mA from 5° to 35° 2θ values and analyzed using PDXL2 software (Rigaku)
- Chemical bond changes: FTIR: IR AFFINITY I - FTIR Spectrophotometer, FTIR 7600, Shimadzu; and JASCO FT-IR 4200 plus spectrophotometer with ATR (range 4000-400 cm^{-1} at 298 K)
- Configuration: TEM*:* FEI Technai Spirit G2, HT 120KV, Electron source LaB6, Netherlands
- Proton resonances: Proton nuclear magnetic resonance (1H-NMR)*:* 300 MHz AVANCE II spectrometer with 5mm BBO probe, recorded at 298.15 K using the standard pulse sequence library of TopSpin 3.2, data processed by TopSpin 3.2 software, of Bruker Biospin, Switzerland.
- Contour and signal-to-noise ratio: 3D fluorescence spectroscopy*:* 3D Fluorescence spectra were measured on a Hitachi F-7000 spectrophotometer in the range of 200-700 nm (fluorescence) at 298 K. The spectral patterns were analyzed using original software (Hitachi).

Result

Agar well diffusion test

MIRGA enhanced the antibiotics' potency by 5-173% compared to control (Figure 1) (Table 1).

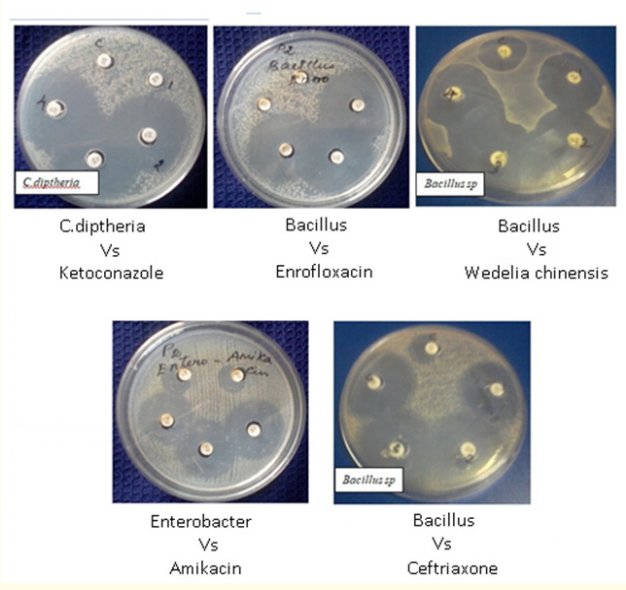

Figure 1: Agar well diffusion method (sample images).

Certain interesting results observed in this study are,

- Antifungal ketoconazole was challenged with *C. diphtheria*. ZOI for control and MIRGA Sprayed are 0 mm and 24 mm receptively.
- Antifungal Amphotericin B was challenged with *E. coli*. The ZOI for control and MIRGA sprayed are 0 mm and 27 mm respectively.
- Enrofloxacin was challenged with *Bacillus sp*. The ZOI for control and MIRGA sprayed are 0 mm and 39 mm respectively.
- Lawsonia inermis was challenged with *Enterobacter sp*. The ZOI for control and MIRGA Sprayed are 0 mm and 14 mm respectively.
- Norfloxacin was challenged with mastitis cow's milk. Treatment of mastitis with norfloxacin is Unusual. The ZOI for control and MIRGA sprayed are 15 mm and 41 mm respectively. This is the highest ZOI (173%) in this study.

Sample No.	Medium	Organism or inoculum	Antibiotic or antiseptic	Zone of inhibition (ZOI) (in mm)					Maximum potentiation (%)
				Control	No. of sprayings				
					1	2	3	4	
1	Nutrient Agar Medium	Ampicillin-resistant *E.coli*	Cloxacillin (10 µg)	15	12	13	14	16	6
2	Nutrient Agar Medium	Clinical mastitis cow's milk	Norfloxacin (10 µg)	15	41	25	30	31	173
3	Mueller-Hinton Agar Medium	*Salmonella sp.*	Amikacin (30 µg)	21	25	29	26	27	38
4	Mueller-Hinton Agar Medium	*Citrobacter diversus*	Ketoconazole (10 µg)	12	24	9	24	20	100
5	Mueller-Hinton Agar Medium	*Pseudomonas sp.*	Chlorohexidine gluconate (20 µL per disc)	11	20	21	22	25	127
6	Mueller-Hinton Agar Medium	*Bacillus sp.*	Enrofloxacin (5 µg)	15	30	30	36	40	166
7	Mueller-Hinton Agar Medium	*Salmonella sp.*	Tincture of iodine (20 µL per disc)	10	16	17	18	19	90
8	Mueller-Hinton Agar Medium	*Staphylococcus aureus*	Chloroxylenol (20 µL per disc)	10	20	21	20	16	110
9	Mueller-Hinton Agar Medium	*Enterobacter sp.*	*Azadirachta indica* (30µL of methanol leaf extract)	12	21	21	14	24	100
10	Mueller-Hinton Agar Medium	*Bacillus sp.*	*Wedelia chinensis* (30µL of methanol leaf extract)	10	14	16	18	18	80
11	Mueller-Hinton Agar Medium	*C. diptheria*	Ketoconazole (10 µg)	No ZOI	No ZOI	23	24	23	Extraordinary potentiation
12	Mueller-Hinton Agar Medium	*Bacillus sp.*	Oxytetracycline–30 µg	15	20	32	26	25	113
13	Mueller-Hinton Agar Medium	*E.coli*	Amphotericin B (20 µg)	No ZOI	27	No ZOI	No ZOI	10	Extraordinary potentiation
14	Mueller-Hinton Agar Medium	*Salmonella sp.*	Ceftriaxone (30 µg per disc)	10	15	20	18	19	100
15	Mueller-Hinton Agar Medium	*Bacillus sp.*	Enrofloxacin (5 µg per disc)	No ZOI	11	39	39	39	Extraordinary potentiation
16	Mueller-Hinton Agar Medium	*Enterobacter sp*	*Lawsonia inermis* (30µL of methanol leaf extract)	No ZOI	11	12	14	14	Extraordinary potentiation
17	Nutrient Agar Medium	Clinical mastitis cow's milk	Amikacin (30 µg)	27	28	32	34	28	26
18	Nutrient Agar Medium	*E. coli*	Oxytetracycline (30 µg)	20	21	20	20	20	5

Table 1: Potentiation of MIRGA sprayed Oxytetracycline against different bacteria as determined by the well diffusion method.

Extraordinary Potentiation means no ZOI in control but extraordinary ZOI in sprayed samples.

More than thousands of such trials were conducted with appropriate control and repeats.

Sensory scores

Two MIRGA spraying enhanced the sweetness, 6 spraying increased the bitterness and 12 sprayings had extremely increased bitterness and sweetness when compared to the control. Notably, these sensory attribute changes were perceived in 1-5 minutes of spraying. The control samples, 6 sprayed and 12 sprayed samples were subjected to various instrumentations, and their results followed.

Instrumentation results

GC-MS

Control contains many heterocyclic compounds, fatty acid derivatives, and long-chain fatty acids such as palmitoleic acid. The main component is hydroxymethylfurfural (2-Furancarboxaldehyde, 5-(hydroxymethyl)-), which is a degradation product of sugars. In 2 sprayed samples, the concentration of that molecule decreases but reaches its maximum upon 6 sprayings. Decreasing again with an excess of spraying i.e., in 12 sprayed samples. The augmentation of the bitterness in 6 sprayed samples could be directly related to the increase of hydroxymethylfurfural because this molecule is from the degradation of sugars. The lower concentration of sugars leads to a reduced sweetness, and bitterness produced by other substances present in the sample is dominant.

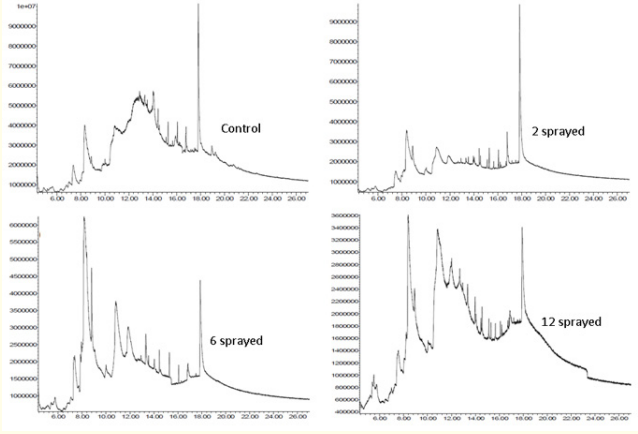

Figure 2: GCMS spectra of Oxytetracycline.

R.T. (Min)	Name of Compound	% Area present in each sample				
		Control	2 sprayed	6 sprayed	12 sprayed	Remarks
5.544	2-Propanone, 1,3-dihydroxy-	0.0	0.0	0.0	7.18	Unique peak in 12 sprayed sample
7.387	4H-Pyran-4-one, 2,3-dihydro-3,5-dihydroxy-6-methyl-	13.6	0.0	0.0	0.0	
7.406	4H-Pyran-4-one, 2,3-dihydro-3,5-dihydroxy-6-methyl-	0.0	0.0	6.47	0.0	
7.490	4H-Pyran-4-one, 2,3-dihydro-3,5-dihydroxy-6-methyl-	0.0	6.62	0.0	0.0	
7.569	4H-Pyran-4-one, 2,3-dihydro-3,5-dihydroxy-6-methyl-	0.0	0.0	0.0	6.70	
8.222	2-Furancarboxaldehyde, 5-(hydroxymethyl)-	0.0	0.0	51.87	0.0	Most abundant peak in 6 sprayed sample
8.344	2-Furancarboxaldehyde, 5-(hydroxymethyl)-	39.18	0.0	0.0	0.0	Most abundant peak in control
8.407	2-Furancarboxaldehyde, 5-(hydroxymethyl)-	0.0	0.0	0.0	32.08	Most abundant peak in 12 sprayed sample
8.409	2-Furancarboxaldehyde, 5-(hydroxymethyl)-	0.0	33.42	0.0	0.0	Most abundant peak in 2 sprayed sample
10.840	α-D-Glucopyranoside, O-α-D-glucopyranosyl-(1.fwdarw.3)-β-D-fructofuranosyl	0.0	0.0	15.19	0.0	
10.862	α-D-Glucopyranoside, O-α-D-glucopyranosyl-(1.fwdarw.3)-β-D-fructofuranosyl	0.0	0.0	0.0	24.03	Unique peak in 12 sprayed sample
10.916	α-D-Glucopyranoside, O-α-D-glucopyranosyl-(1.fwdarw.3)-β-D-fructofuranosyl	0.0	20.17	0.0	0.0	
11.872	α-D-Glucopyranoside, O-α-D-glucopyranosyl-(1.fwdarw.3)-β-D-fructofuranosyl	0.0	0.0	8.47	0.0	Unique peak in 6 sprayed sample

12.040	α-D-Glucopyranoside, O-α-D-glucopyranosyl-(1. fwdarw.3)-β-D-fructofuranosyl	0.0	0.0	0.0	7.19	Unique peak in 12 sprayed sample
12.721	α-D-Glucopyranoside, O-α-D-glucopyranosyl-(1. fwdarw.3)-β-D-fructofuranosyl	0.0	0.0	0.0	3.24	
13.347	Propan-1-one, 2-methylthio-1-phenyl-, oxime	0.0	0.0	3.10	0.0	Unique peak in 6 sprayed sample
13.374	α-D-Glucopyranoside, O-α-D-glucopyranosyl-(1. fwdarw.3)-β-D-fructofuranosyl	0.0	0.0	0.0	1.33	
13.990	Tridecanoic acid, 3-hydroxy-, ethyl ester	0.0	3.84	0.0	0.0	
13.994	Tridecanoic acid, 3-hydroxy-, ethyl ester	0.0	0.0	0.0	1.18	
14.477	Tridecanoic acid, 3-hydroxy-, ethyl ester	0.0	2.99	0.0	0.0	
14.478	[1,1'-Bicyclopropyl]-2-octanoic acid, 2'-hexyl-, methyl ester	9.16	0.0	0.0	0.0	
14.481	Tridecanoic acid, 3-hydroxy-, ethyl ester	0.0	0.0	1.09	0.0	
14.586	Tridecanoic acid, 3-hydroxy-, ethyl ester	0.0	0.0	0.0	1.76	
15.153	Tridecanoic acid, 3-hydroxy-, ethyl ester	0.0	0.0	0.0	2.75	
15.314	1b,4a-Epoxy-2H-cyclopenta[3,4]cyclopro-pa[8,9]cycloundec[1,2-b]oxiren-5(6H)-one, 7-(acetyloxy)decahydro-2,9,10	0.0	0.0	0.0	5.21	
15.314	9,12,15-Octadecatrienoic acid, 2-[(trimethyl-silyl)oxy]-1-[[(trimethylsilyl)oxy]methyl]ethyl ester, (Z,Z,Z)-	0.0	3.20	0.0	0.0	
15.317	α-D-Glucopyranoside, methyl 2-(acetylamino)-2-deoxy-3-O-(trimethylsilyl)-, cyclic methylboronate	0.0	0.0	0.61	0.0	
16.088	9,12,15-Octadecatrienoic acid, 2-[(trimethyl-silyl)oxy]-1-[[(trimethylsilyl)oxy]methyl]ethyl ester, (Z,Z,Z)-	0.0	1.11	0.00	0.0	
16.090	1b,4a-Epoxy-2H-cyclopenta[3,4]cyclopro-pa[8,9]cycloundec[1,2-b]oxiren-5(6H)-one, 7-(acetyloxy)decahydro-2,9,10-trihydroxy	5.30	0.0	0.0	0.0	
16.097	α-D-Glucopyranoside, methyl 2-(acetylamino)-2-deoxy-3-O-(trimethylsilyl)-, cyclic methylboronate	0.0	0.0	0.63	0.0	
16.813	14-Octadecenal	7.66	0.0	0.0	0.0	
16.814	9-Octadecenamide	0.0	4.93	0.0	0.0	
17.838	9-Octadecenamide	16.07	0.0	0.0	0.0	Unique peak in control
17.851	9-Hexadecenoic acid	0.0	23.72	0.0	0.0	Unique peak in 12 sprayed sample
17.889	9-Octadecenamide	0.0	0.0	12.57	0.0	Unique peak in 6 sprayed sample
17.927	cis-11-Eicosenamide	0.0	0.0	0.0	12.42	Unique peak in 12 sprayed sample
18.967	γ-Sitosterol	3.83	0.0	0.0	0.0	

Table 2: GC-MS spectra analysis.

Powder XRD

Patterns showed that the samples were highly polycrystalline. From Table 3, sprayed samples have diffraction patterns similar to the control sample; however different 2θ angles are observed for maximum intensity peaks. The maximum intensity for each pattern is observed at 2θ: 18.80 (control), 24.75 (2 sprayed), 19.62 (6 sprayed), and 24.75 (12 sprayed). These intensity variations are evidence of an atomic rearrangement in the diffraction planes due to isostructural polymorphs induced by MIRGA-generated mid-IR.

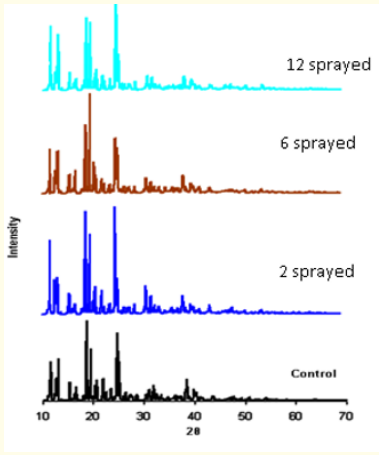

Figure 3: PXRD spectra of Oxytetracycline.

	(I/Imax)%			
2θ	**Control**	**2 sprayed**	**6 sprayed**	**12 sprayed**
18.80	100	66	47	61
24.75	85	100	52	100
19.62	65	66	100	60
13.17	53	34	32	58
11.69	49	69	45	69
25.18	49	30	36	32

Table 3: PXRD peaks analysis of Oxytetracycline.

FTIR

- **Instrument:** IR AFFINITY I - FTIR Spectrophotometer, FTIR 7600, Shimadzu (Figure 4a). Oxytetracycline concentration was found to be higher in 6 sprayed samples.
- **Instrument:** JASCO FT-IR 4200 plus spectrophotometer with ATR (range 4000-400 cm^{-1} at 298 K) (Figure 4b).

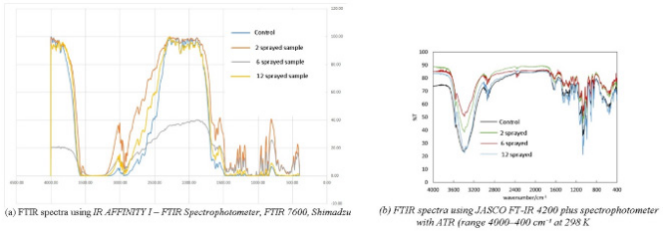

Figure 4: FTIR spectra of Oxytetracycline.

Control Sample: The relatively sharp peak at 2935 cm^{-1} as well as the broad signal in the range of 3200-3600 cm^{-1} seen amongst others in the functional group region are respectively associated with the stretching vibrations of C-H and of O-H in oxytetracycline powder. Furthermore, the very weak signal at 2360 cm^{-1} is associated with -N = C = N, -C = N, -N = C, -N = C = O bonds.

2 sprayed sample: No significant change in the fingerprint region compared to the control sample. In the functional group region, however, in addition to a shift in the background signal the C-H stretching vibration[24] at 2935 cm^{-1} dropped by around 3% compared to the control sample. Furthermore, the O-H stretching vibration at 3200-3600 cm^{-1} dropped by around 20%. Conversely, the very weak -N = C = N, -C = N, -N = C, -N = C = O signal at 2360 cm^{-1} raised by around 5%.

6 sprayed sample: Following the same trend in the 2 sprayed samples, in the fingerprint region the C-H stretching vibration [27] at 2935 cm^{-1} dropped by around 3% compared to the control sample. Furthermore, the O-H stretching vibration at 3200-3600 cm^{-1} dropped by a further 10%. Conversely, the very weak -N = C = N, -C = N, -N = C, -N = C = O signal at 2360 cm^{-1} raised by further 5%.

12 sprayed samples: No significant change in the fingerprint region compared to the control and 2 sprayed samples. In the functional group region, however, in addition to a shift in the background signal, the C-H stretching vibration [27] at 2935 cm^{-1} increased again such that it was around 4% higher than the control sample. Furthermore, the O-H stretching vibration at 3200-3600 cm^{-1} increased again such that it was around 10% higher than the control sample and dropped by about 20% in the 6 sprayed samples compared to the control. The signal raised again in the 12 sprayed samples such that it was around 10% higher than the control sample. Conversely, the very weak signal at 2360 cm^{-1} shifts

from absorption behavior to transmission behavior indicating a complex response of the -N = C = N, -C = N, -N = C, -N = C = O bonds in oxytetracycline powder due to MIRGA emitted mid-IR.

The average transmission signal peaked as the spraying increased from 2 to 6 but dropped at 12 sprayings. Also observed were C-H and O-H stretching vibrations, as well as the switching of the absorption to the transmission in -N = C = N, -C = N, -N = C, -N = C = O bonds. Therefore, the overall absorption by the sprayed samples in the mid-IR spectrum is a mix and complex behavior depending on the number of sprayings. Also, comparatively oxytetracycline concentration was found more in the sample exposed to 6 sprayings. This suggests that for clinical use, samples exposed to 2 and 6 sprays are favorable than the control and an exposure of 12 sprayings is unfavorable.

HR-TEM

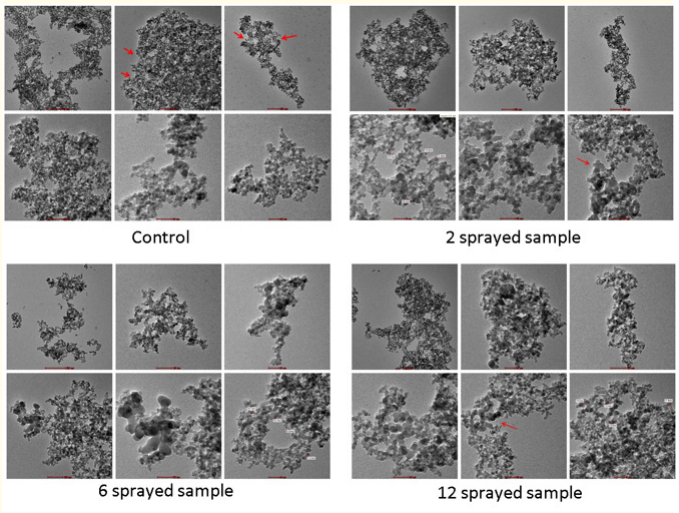

Figure 5: TEM images of Oxytetracycline.

Control: Nanoparticle clusters show differences concerning size, shape, and spatial arrangement. Three main arrangements of nanoparticles are observed, that determine the cluster shape: hole type, ball/tangle type, and elongated type. Clusters are sized, on average: 2 - 10 µm (perimeter) and 0.5 - 2 µm (main diameter), and include a variable number of holes (2 - 10, roughly, depending on the overall cluster size) having diameters in the range 50 - 100 nm. Each cluster is formed by a very large number of nanoparticles (order of thousands), strongly overlapping each other. Nanoparticle sizes show narrow variability, that is 5 - 10 nm and prevalent prolate ellipsoidal shape; size becomes homogeneous either within the same cluster or among different clusters. Nanoparticles do not show crystalline structure.

2 sprayed sample: Nanoparticles are the only particulate component. 2 sprayed sample is significantly similar to the control with respect to the size and shape of clusters, holes in clusters, and nanoparticles including the degree of their reciprocal overlapping in the cluster. Concerning cluster shape, however, in the 2 sprayed samples the hole type is not observed, while the other two types (ball/tangle and elongated) are documented. Clusters have perimeters ranging from 5 - 10 µm, as for images where clusters are entirely visible, and diameters ranging from 1 - 2 µm. Holes are in comparable number, by each cluster, to the control sample, and are sized 0.05 - 0.2 µm diameter. Nanoparticles range from 10 - 20 nm, as also documented by the bottom left image and ellipsoidal shape. However, a small number of larger nanoparticles, sized 20 - 40 nm, is observed in 2 sprayed sample that is almost absent in the control.

6 sprayed sample: Clusters of nanoparticles are the only particulate component. Similarities mainly concern the size and shape of clusters, holes in clusters, and nanoparticles including the degree of reciprocal particle overlapping in the clusters. Concerning clusters, the hole type is not observed, while the other two types (ball/tangle and elongated) are documented; in addition, a fragmented arrangement is observed. In the fragmented arrangement, the size of fragments is lower than previously observed, although the size of the overall arrangement is comparable (1.5 - 2 µm). Nevertheless, the clusters observed are generally smaller than in 2 sprayed samples. For example, the perimeters of clusters in the top central (ball/tangle type) and right (elongated type) images, are roughly 1.5 and 2.5 µm, while diameters are 0.5 and 1 µm, respectively. Similarly, holes are smaller as well, with diameters ranging from 0.05 - 0.1 µm and they also are in smaller numbers by cluster. Concerning nanoparticles, their size and shape are comparable to those of previous samples, that is 10 - 20 nm size and ellipsoidal shape. Larger nanoparticles are also observed ranging from 30 - 60 nm Nanoparticles do not show crystalline structure.

12 sprayed sample: Clusters of nanoparticles are the only particulate type observed. Nanoparticles are strongly overlapped each other and are in the order of thousands by cluster. Their size ranges 10 - 20 nm and shapes range from spherical to ellipsoidal. Concerning clusters, two ball/tangle and elongated types are observed. Sizes are however more variable than previously observed. Holes are observed in clusters, of similar sizes than in previous samples, although their number by cluster seems lower. Larger nanoparticles ranging from 20 - 40 nm are observed.

More evident differences are observed in the cluster shapes, particularly concerning the 6 sprayed samples when compared to other samples.

Proton NMR

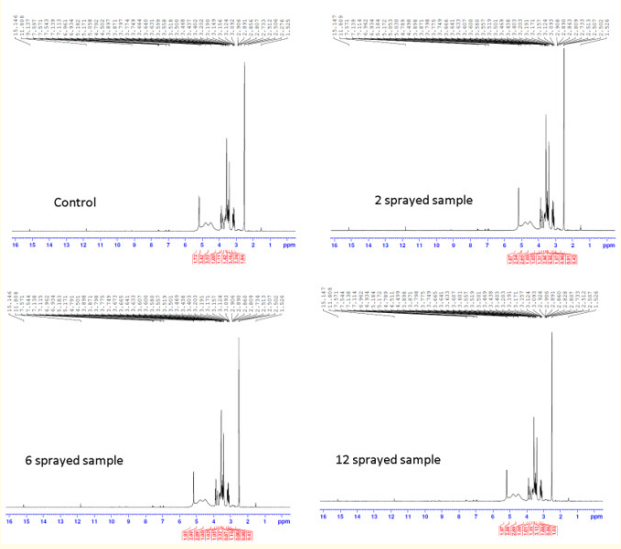

Figure 6: Proton NMR spectra of Oxytetracycline.

Proton resonances are detected. A study has reported that oxytetracycline has a bitter taste [28,29]. In 2 sprayed samples, it is possible that resonances in the region where sugar-like molecules were detected had given the sweetness, for example, H-1 NMR spectroscopy chemical shifts of glucose are in the range of ~3.2 to ~5.2 ppm, the H-1 shifts for sucrose are from ~3.5 to ~4.5 ppm, and those of fructose are in the range of ~3.6 ppm to ~4.1 ppm. NMR resonances recorded were C = C-H, Phenol, Aromatic-NH (5.2 doublet, 4.8 broad peak, 4.5 broad peak), HCO, OH, NH (3.9 doublet, 3.8 triplet, ~3.6 mult.), OH, NH (3.2 quartet) and HCN (2.5 singlet).

3D fluorescence spectroscopy

Four plots are characterized by island contours centered at (Ex = 547 nm, Em = 700 nm) and (453 nm, 551 nm), while a plateau is observable at regions (Ex = 314 nm - 419 nm, Em = 353 nm - 517 nm). When the excitation is in the 200 nm - 260 nm UV region, there is a strong fluorescence signal encompassing almost all the visible range (250 nm - 750 nm). The fluorescence fingerprint of the control, 2, 6, and 12 sprayed samples (with the increased number of sprayings) showed more variation in the contour indicating a change in the signal-to-noise ratio.

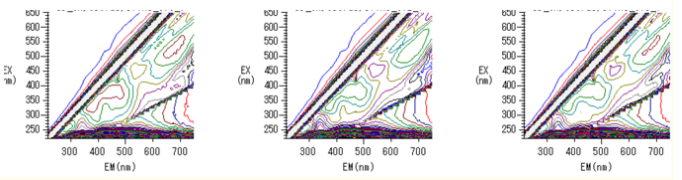

Figure 7: 3D fluorescence spectra of Oxytetracycline.

Discussion

Antibiotic potentiation and potentiators

Potentiation is the process of intensifying the effect of one chemical by another chemical [30]. An antibiotic potentiator is a substance that need not have antimicrobial activity itself but that yields a synergistic effect to classical antimicrobials when used in combination. In other words, a potentiator will act as an antimicrobial adjuvant.

Presently available antibiotic potentiators are co-administered with antibiotics to enhance the antimicrobial action. These types of enhancing compounds possess many advantages but act selectively on specific antibiotics and against certain bacteria [31]. Other limitations often include drug-to-drug interaction risk and inappropriate co-dosing [32-34]. The prediction of drug combinations is of great clinical significance [35]. The demand for discovering a safe, broad-spectrum adjuvant to potentiate a wide range of antibiotics is a vital and urgent need. One such alternative has been identified in this study with the use of mid-IR. It was shown that 2-6 µm mid-IR generated from the MIRGA has potentiated the commonly used antibiotics. Thereby making chances to reduce the clinical dose used against viz., *E. coli, Salmonella, Citrobacter, Pseudomonas, Bacillus, Staphylococcus, and Enterobacter.*

The invention background, definition, technique of mid-IR generation from MIRGA, toxicological study on MIRGA, the safety of the MIRGA sprayed usable and primeval, and future scope of MIRGA have been described by [11-13] (Detailed discussion in the supplementary file: Text T1).

The inorganic compounds used in the generation of MIR are a perspective for biomedical applications [36,37]. It is also a new synthesis method for the preparation of functional material (2-6 µm mid-IR) [38,39]. It is well known that the combination of different compounds, which have excellent electronic properties, leads to new composite materials, which have earned great technological interest in recent years [40,41].

Action of 2-6 µm mid-IR on Oxytetracycline

2-6 µm mid-IR is non-ionizing, non-carcinogenic [42], safe even to the eyes [43], and can penetrate obscurants [22,44]. Thus, the mid-IR generated from MIRGA penetrates the package and falls on the inside oxytetracycline. The oxytetracycline molecules absorb the mid-IR and elicit vibrational oscillations, which lead to the stretching and bending of chemical bonds in the molecules [45]. The altered chemical bonds lead to a change in the molecular configuration, thereby the physicochemical nature, i.e. the potency of the oxytetracycline is augmented [46-48]. Instrumentation results of the oxytetracycline have witnessed these molecular changes, thereby illustrating the action of mid-IR in potentiating the efficacy of antibiotics.

Though MIRGA spraying altered the antibiotic's chemical structure, it still acts on the bacteria. This action can be compared and similar to e.g., quinolones and cephalosporins. In cephalosporins, 7-ACA side chain modification leads to potentiated multiple antibiotics. Various substitutions on the basic quinolone structure yielded potentiated multiple antibiotics. In penicillin, tetracyclines, sulphanamides, macrolides, aminoglycosides, and potentiated multiple derivatives are developed by altering the chemical structure [49].

Future perspectives with MIRGA-potentiated antibiotics

- With the enhanced antibiotics' potency, the therapeutic dose, economy, and host stress can be reduced, and resource-saving.
- Reduced drug dose would reduce excretion and hence reduce environmental pollution.
- Side effects from the antibiotics can be reduced due to lower doses.
- A revival of the potency of antibiotics that have lost or are losing (e.g., penicillin) can be achieved.
- One-time spraying for a strip of antibiotic tablets or a bottle of syrup is sufficient and need not be sprayed for every time use.
- Currently hundreds of antibiotics have been developed over time to overcome the consistently developing microbial resistance, and each has its side effects and cost ineffectiveness. In the future, a few classes of MIRGA-sprayed antibiotics might be enough to treat living beings for a longer period (A probable future scope of using MIRGA in antibiotic resistance is presented in the supplementary file: Text T2).

Conclusion

We have tested the applicability of 2-6 µm mid-IR emitted from a specially designed, pocket-sized mid-IR generating atomizer (MIRGA) to potentiate antibiotics. It was shown that the potency of the antibiotics was enhanced over a range of 5 to 173%. This technology is more effective than the existing methods to overcome antimicrobial resistance and minimize the dose, economy, and host stress. This research may help to enhance the potency of other pharmaceuticals, especially the costliest.

Funding

This study received no specific funding.

Conflict of Interest

By the journal's policy and our ethical obligation as researchers, we submit that the authors Dr.Umakanthan and Dr.Madhu Mathi are the inventors and patentee of the Indian patent for MIRGA (patent no.: 401387) which is a major material employed in this study.

Data and Materials Availability

All data is available in the manuscript and supplementary materials.

Author Contributions

- Umakanthan: Conceptualization, Methodology, Supervision, Validation, Funding.
- Madhu Mathi: Investigation, Data curation, Visualization, Writing - Original draft preparation.
- Umadevi, Sivaramakrishnan: Project administration, Resources, Writing- Reviewing and Editing.

Ethics Approval, Consent to Participate, Consent for Publication

Not Applicable.

Bibliography

1. Eliopoulos G M and C T Eliopoulos. "Antibiotic combinations: should they be tested?". *Clinical Microbiology Reviews* 1.2 (1988): 139-156.

2. Zimmermann Grant R., *et al*. "Multi-target therapeutics: when the whole is greater than the sum of the parts". *Drug Discovery Today* 12.1-2 (2007): 34-42.

3. Bassetti Matteo and Elda Righi. "New antibiotics and antimicrobial combination therapy for the treatment of gram-negative bacterial infections". *Current Opinion in Critical Care* 21.5 (2015): 402-411.

4. Bassetti Matteo., *et al*. "Antimicrobial resistance and treatment: an unmet clinical safety need". *Expert Opinion on Drug Safety* 17.7 (2018): 669-680.

5. Roell Kyle R., *et al*. "An introduction to terminology and methodology of chemical synergy—perspectives from across disciplines". *Frontiers in Pharmacology* 8 (2017): 158.

6. Petrosillo, Nicola, *et al*. "Management of antibiotic resistance in the intensive care unit setting". *Expert Review of Anti-Infective Therapy* 8.3 (2010): 289-302.

7. Ahmed Armin., *et al*. "Current concepts in combination antibiotic therapy for critically ill patients". *Indian Journal of Critical Care Medicine: Peer-Reviewed, Official Publication of Indian Society of Critical Care Medicine* 18.5 (2014): 310.

8. Argyraki Aikaterini., *et al*. "UV light assisted antibiotics for eradication of in vitro biofilms". *Scientific Reports* 8.1 (2018): 16360.

9. Kirui Dickson K., *et al*. "Targeted laser therapy synergistically enhances efficacy of antibiotics against multi-drug resistant Staphylococcus aureus and Pseudomonas aeruginosa biofilms". *Nanomedicine: Nanotechnology, Biology and Medicine* 20 (2019): 102018.

10. Balan Vera, *et al*. "Vibrational spectroscopy fingerprinting in medicine: from molecular to clinical practice". *Materials* 12.18 (2019): 2884.

11. Umakanthan Mathi M. "Decaffeination and improvement of taste, flavor and health safety of coffee and tea using mid-infrared wavelength rays". *Heliyon* 8.11 (2022).

12. Thangaraju Umakanthan and Madhu Mathi. "Quantitative reduction of heavy metals and caffeine in cocoa using mid-infrared spectrum irradiation". *Journal of the Indian Chemical Society* 100.1 (2023): 100861.

13. Umakanthan Thangaraju and Madhu Mathi. "Increasing saltiness of salts (NaCl) using mid-infrared radiation to reduce the health hazards". *Food Science and Nutrition* (2023).

14. Ashcroft Frances. "Life at the extremes: the science of survival". Univ of California Press, (2002): 122.

15. Sanders Robert H. "Revealing the Heart of the Galaxy". Cambridge University Press, (2014): 70

16. Verheest Frank. "Waves in dusty space plasmas". Vol. 245. Springer Science and Business Media, (2000): 89.

17. Keping Sun and Gefei Yu. "Applied Electrostatics (ICAES 2004): Proceedings of the Fifth International Conference on Applied Electrostatics". Elsevier, (2004): 87.

18. Fauchais Pierre L., *et al*. "Thermal spray fundamentals: from powder to part". Springer Science and Business Media, (2014): 84.

19. Pople S. "Complete Physics". Oxford University Press, Oxford, (1999): 166.

20. Singh KC. "Basic Physics". PHL Learning Private Limited, New Delhi, (2009): 413.

21. Wendisch Manfred and Jean-Louis Brenguier. "Airborne measurements for environmental research: methods and instruments". John Wiley andd Sons, (2013).

22. Prasad M Soul. God and Buddha in Language of Science, Notion Press, Chennai, (2017).

23. Aboud Salam A., *et al*. "A comprehensive review on infrared heating applications in food processing". *Molecules* 24.22 (2019): 4125.

24. Murray P R., *et al*. "Manual of Clinical Microbiology". 6th Ed. ASM Press, Washington DC, (1995): 15-18.

25. Everitt, Margaret. "Consumer-targeted sensory quality". *Global Issues in Food Science and Technology* Academic Press, (2009): 117-128.

26. Wichchukit Sukanya and Michael O'Mahony. "The 9-point hedonic scale and hedonic ranking in food science: some reappraisals and alternatives". *Journal of the Science of Food and Agriculture* 95.11 (2015): 2167-2178.

27. Socrates George. "Infrared and Raman characteristic group frequencies: tables and charts". John Wiley and Sons, (2004).

28. Uchida Takahiro., *et al*. "Evaluation of the bitterness of antibiotics using a taste sensor". *Journal of Pharmacy and Pharmacology* 55.11 (2003): 1479-1485.

29. Yang Wangrong., *et al*. "TetX is a flavin-dependent monooxygenase conferring resistance to tetracycline antibiotics". *Journal of Biological Chemistry* 279.50 (2004): 52346-52352.

30. Engs Ruth Clifford. "Alcohol and other drugs: self-responsibility". Tichenor Pub., (1987).

31. Goodman Louis Sanford. "Goodman and Gilman's the pharmacological basis of therapeutics". Vol. 1549. New York: McGraw-Hill, (1996): 68.

32. Allen Richard C and Sam P Brown. "Modified antibiotic adjuvant ratios can slow and steer the evolution of resistance: co-amoxiclav as a case study". *Mbio* 10.5 (2019): 10-1128.

33. Wassmann Claes Søndergaard., *et al*. "Cannabidiol is an effective helper compound in combination with bacitracin to kill Gram-positive bacteria". *Scientific Reports* 10.1 (2020): 4112.

34. Song Meirong, *et al*. "A broad-spectrum antibiotic adjuvant reverses multidrug-resistant Gram-negative pathogens". *Nature Microbiology* 5.8 (2020): 1040-1050.

35. Pan Yichen., *et al*. "Review of Predicting Synergistic Drug Combinations". *Life* 13.9 (2023): 1878.

36. Dukenbayev Kanat., *et al*. "Fe3O4 nanoparticles for complex targeted delivery and boron neutron capture therapy". *Nanomaterials* 9.4 (2019): 494.

37. Tishkevich D I., *et al*. "Immobilization of boron-rich compound on Fe3O4 nanoparticles: stability and cytotoxicity". *Journal of Alloys and Compounds* 797 (2019): 573-581.

38. Kozlovskiy Artem L., *et al*. "Study of the effect of ion irradiation on increasing the photocatalytic activity of WO 3 microparticles". *Journal of Materials Science: Materials in Electronics* 32 (2021): 3863-3877.

39. El-Shater Reda E., *et al*. "Synthesis, characterization, and magnetic properties of Mn nanoferrites". *Journal of Alloys and Compounds* 928 (2022): 166954.

40. Kozlovskiy A L and M V Zdorovets. "Effect of doping of Ce4+/3+ on optical, strength and shielding properties of (0.5-x) TeO2-0.25 MoO-0.25 Bi2O3-xCeO2 glasses". *Materials Chemistry and Physics* 263 (2021): 124444.

41. Almessiere M A., *et al*. "Investigation of exchange coupling and microwave properties of hard/soft (SrNi0. 02Zr0. 01Fe11. 96O19)/ (CoFe2O4) x nanocomposites". *Materials Today Nano* 18 (2022): 100186.

42. Ilev I K and R W Waynant. "Mid-infrared biomedical applications". *Mid-infrared Semiconductor Optoelectronics* (2006): 615-634.

43. Barh Ajanta., *et al*. "Thermally controlled mid-IR band-gap engineering in all-glass chalcogenide microstructured fibers: a numerical study". *Journal of Optics* 19.6 (2017): 065603.

44. Pereira Mauro F and Oleksiy Shulika. "Terahertz and mid infrared radiation: generation, detection and applications". Springer, (2011).

45. Guerrero-Pérez M Olga and Gregory S Patience. "Experimental methods in chemical engineering: Fourier transform infrared spectroscopy—FTIR". *The Canadian Journal of Chemical Engineering* 98.1 (2020): 25-33.

46. Flynn George W., *et al*. "Vibrational energy transfer". *The Journal of Physical Chemistry* 100.31 (1996): 12817-12838.

47. Yi Gyu-Chul. "Semiconductor nanostructures for optoelectronic devices: Processing, characterization and applications". Springer Science and Business Media, (2012): 198.

48. Ruren Xu and Yan Xu. "Modern Inorganic Synthetic Chemistry". 2nd edn., Elsevier B.V, Netherlands, UK, USA, (2017): 124.

49. Guo Zongru. "The modification of natural products for medical use". *Acta Pharmaceutica Sinica B* 7.2 (2017): 119-136.